Applying Computational Methods to Determine the Electric Current Density in a MHD Generator Channel from External Flux Density Measurements

V. A. Bokil[1], **N. L. Gibson**[1], D. A. McGregor[1,2], C. R. Woodside[2]

(1) Oregon State University
(2)National Energy Technology Laboratory

Pacific Coast Carbon Storage / Computational Energy Science Research Closeout Meeting

October 29, 2014

Finding Arcs in MHD Generators

V. A. Bokil[1], **N. L. Gibson**[1], D. A. McGregor[1,2], C. R. Woodside[2]

(1) Oregon State University
(2)National Energy Technology Laboratory

Pacific Coast Carbon Storage / Computational Energy Science Research
Closeout Meeting

October 29, 2014

Outline

Outline

Outline

Outline

Outline

Outline

Outline

1. **Introduction**
2. Inverse Problem
3. Modeling
4. Simulation
5. Sensitivity Analysis
6. Conclusions

Magneto-hydrodynamic Power Generation

- Magneto-hydrodynamic (MHD) Power Generation offers significant theoretical efficiency gains over traditional turbo-machinery steam cycles when used as a topping cycle

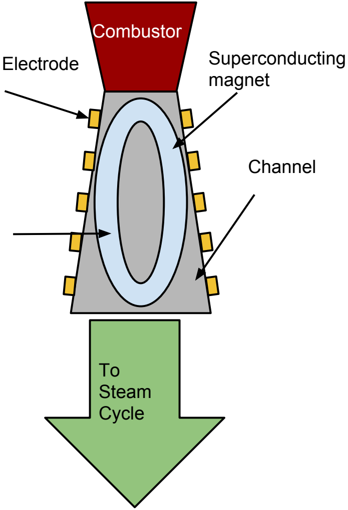

Magneto-hydrodynamic Power Generation

- Magneto-hydrodynamic (MHD) Power Generation offers significant theoretical efficiency gains over traditional turbo-machinery steam cycles when used as a topping cycle
- The combustion product is low conductivity, thermally generated plasma. Passing this plasma through a strong magnetic field near electrodes generates electrical power.

Lorentz Force

$$\mathbf{F} = q(\mathbf{E} + \mathbf{u} \times \mathbf{B})$$

$\mathbf{u}$ = velocity, $\mathbf{E}, \mathbf{B}$ = electric/magnetic fields

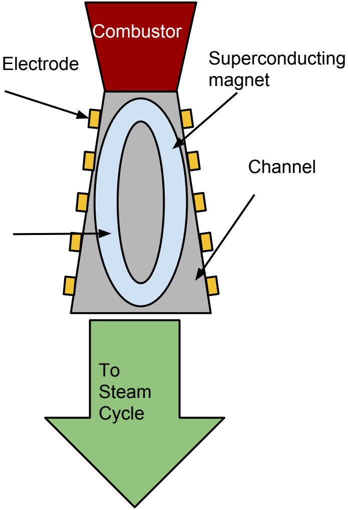

Magneto-hydrodynamic Power Generation

- Magneto-hydrodynamic (MHD) Power Generation offers significant theoretical efficiency gains over traditional turbo-machinery steam cycles when used as a topping cycle
- The combustion product is low conductivity, thermally generated plasma. Passing this plasma through a strong magnetic field near electrodes generates electrical power.
- Efficiency gains are primarily due to the lack of moving parts, which allows for very high temperatures in the generator.

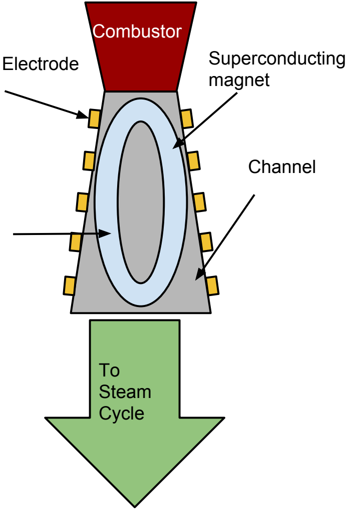

Magneto-hydrodynamic Power Generation

- Magneto-hydrodynamic (MHD) Power Generation offers significant theoretical efficiency gains over traditional turbo-machinery steam cycles when used as a topping cycle
- The combustion product is low conductivity, thermally generated plasma. Passing this plasma through a strong magnetic field near electrodes generates electrical power.
- Efficiency gains are primarily due to the lack of moving parts, which allows for very high temperatures in the generator.
- However, MHD Power Generation suffers from high life-cycle costs due, in part, to high component failure rates inside the channel, potentially caused by "arcing".

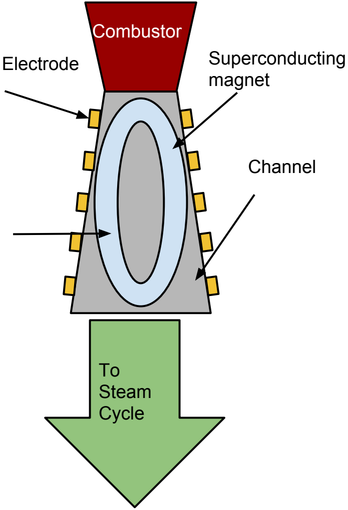

MHD Generator Arcs

- Since the wall of the generator channel is cool relative to the bulk plasma temperature (for example 500° K vs. 2500° K), a thermal boundary layer forms near the wall of the channel.

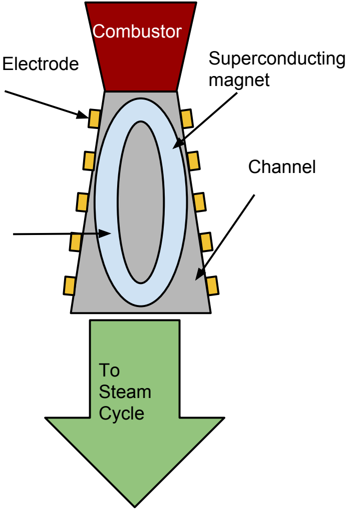

MHD Generator Arcs

- Since the wall of the generator channel is cool relative to the bulk plasma temperature (for example 500° K vs. 2500° K), a thermal boundary layer forms near the wall of the channel.
- The plasma is thermally generated so the conductivity drops dramatically with the plasma temperature.

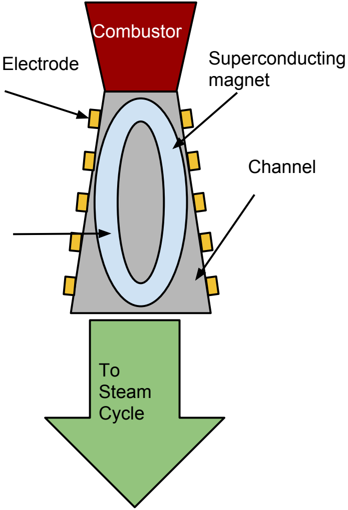

MHD Generator Arcs

- Since the wall of the generator channel is cool relative to the bulk plasma temperature (for example 500° K vs. 2500° K), a thermal boundary layer forms near the wall of the channel.
- The plasma is thermally generated so the conductivity drops dramatically with the plasma temperature.
- However, the total current across the channel is constant, so current will "jump the conductivity gap."

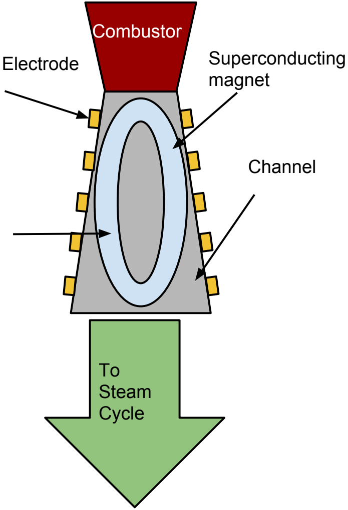

MHD Generator Arcs

- Since the wall of the generator channel is cool relative to the bulk plasma temperature (for example 500° K vs. 2500° K), a thermal boundary layer forms near the wall of the channel.
- The plasma is thermally generated so the conductivity drops dramatically with the plasma temperature.
- However, the total current across the channel is constant, so current will "jump the conductivity gap."
- It does so in very high density **arcs**. These arcs are hot and damage the electrodes, which must be replaced.

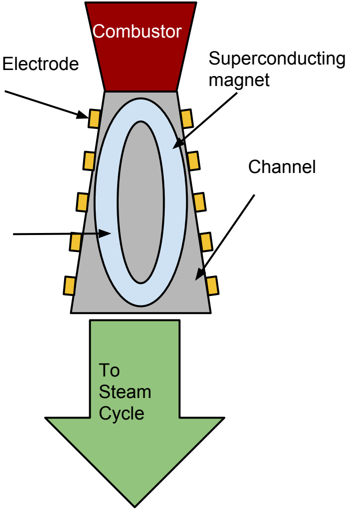

MHD Generator Arcs

- Since the wall of the generator channel is cool relative to the bulk plasma temperature (for example 500° K vs. 2500° K), a thermal boundary layer forms near the wall of the channel.
- The plasma is thermally generated so the conductivity drops dramatically with the plasma temperature.
- However, the total current across the channel is constant, so current will "jump the conductivity gap."
- It does so in very high density **arcs**. These arcs are hot and damage the electrodes, which must be replaced.
- We seek to detect the location of arcs (areas of particularly large current density) from external magnetic flux density measurements.

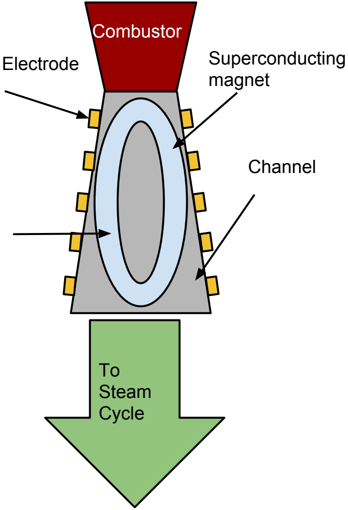

Outline

Reconstruction

- Current densities inside the generator cannot be directly measured due to high temperatures, magnetic fields, and corrosive gasses

Reconstruction

- Current densities inside the generator cannot be directly measured due to high temperatures, magnetic fields, and corrosive gasses
- There is, however, a magnetic field that is induced by the internal electric field, which extends beyond the channel

Reconstruction

- Current densities inside the generator cannot be directly measured due to high temperatures, magnetic fields, and corrosive gasses
- There is, however, a magnetic field that is induced by the internal electric field, which extends beyond the channel
- Measuring internal features by induced magnetic fields has been successfully implemented for Vacuum Arc Remelters

Reconstruction

- Current densities inside the generator cannot be directly measured due to high temperatures, magnetic fields, and corrosive gasses
- There is, however, a magnetic field that is induced by the internal electric field, which extends beyond the channel
- Measuring internal features by induced magnetic fields has been successfully implemented for Vacuum Arc Remelters
- We are interested in Current Reconstruction using external measurements of the induced magnetic flux density

Reconstruction

- Current densities inside the generator cannot be directly measured due to high temperatures, magnetic fields, and corrosive gasses
- There is, however, a magnetic field that is induced by the internal electric field, which extends beyond the channel
- Measuring internal features by induced magnetic fields has been successfully implemented for Vacuum Arc Remelters
- We are interested in Current Reconstruction using external measurements of the induced magnetic flux density
- Typically current reconstruction relies on the solution of *integral equations*, e.g., the **Biot-Savart Law** [1, 2], which involves special assumptions of geometry and/or material parameters

Reconstruction

- Current densities inside the generator cannot be directly measured due to high temperatures, magnetic fields, and corrosive gasses
- There is, however, a magnetic field that is induced by the internal electric field, which extends beyond the channel
- Measuring internal features by induced magnetic fields has been successfully implemented for Vacuum Arc Remelters
- We are interested in Current Reconstruction using external measurements of the induced magnetic flux density
- Typically current reconstruction relies on the solution of *integral equations*, e.g., the **Biot-Savart Law** [1, 2], which involves special assumptions of geometry and/or material parameters
- Instead, we solve a more flexible *differential equations model* and perform a **simulation-based parameter estimation.**

Simulation-Based Parameter Estimation

- We assume a parameterization of the quantity of interest (current density)
- Given external field measurements, we find the minimizer of a discrepancy function involving a simulation (using Newton's method to explore parameter space)
- Requires no special assumptions of geometry or material
- In practice, convergence depends on accuracy of initial estimates
- Need an accurate model of the essential physics, and an efficient numerical simulation method

Non-linear Least Squares

- We aim to perform a least squares fit to data in parameter space (e.g., $\vec{q}$) using a discretization of the PDE to evaluate the discrepancy function.

Non-linear Least Squares

- We aim to perform a least squares fit to data in parameter space (e.g., $\vec{q}$) using a discretization of the PDE to evaluate the discrepancy function.
- Let $\mathcal{A}\mathbf{b} = \mathbf{j}$ represent the mapping from the induced magnetic flux density to the current density. Then $\mathcal{A}^{-1}$ yields the solution of this forward problem.

Non-linear Least Squares

- We aim to perform a least squares fit to data in parameter space (e.g., $\vec{q}$) using a discretization of the PDE to evaluate the discrepancy function.
- Let $\mathcal{A}\mathbf{b} = \mathbf{j}$ represent the mapping from the induced magnetic flux density to the current density. Then $\mathcal{A}^{-1}$ yields the solution of this forward problem.
- Let D be a vector of measurements, $\mathbb{O}$ be a restriction of the discrete solution to the observation location, then a discrepancy function is given by

$$\arg\min_{\vec{q}} \left\| D - \mathbb{O}\left(\mathcal{A}^{-1}\mathbf{j}(\vec{q})\right) \right\|^2$$

Non-linear Least Squares

- We aim to perform a least squares fit to data in parameter space (e.g., $\vec{q}$) using a discretization of the PDE to evaluate the discrepancy function.
- Let $\mathcal{A}\mathbf{b} = \mathbf{j}$ represent the mapping from the induced magnetic flux density to the current density. Then $\mathcal{A}^{-1}$ yields the solution of this forward problem.
- Let D be a vector of measurements, $\mathbb{O}$ be a restriction of the discrete solution to the observation location, then a discrepancy function is given by

$$\arg\min_{\vec{q}} \left\| D - \mathbb{O}\left(\mathcal{A}^{-1}\mathbf{j}(\vec{q})\right) \right\|^2$$

- The forward problem must be solved numerous times until convergence of the optimization scheme

Outline

Away from the walls of the generator the plasma flow is modeled with the compressible Euler equations, while the electromagnetic variables are governed by Maxwell's equations (with appropriate initial and boundary conditions)

$$\rho\left(\partial_t - \mathbf{u}\cdot\nabla\right)\mathbf{u} = \mathbf{j}\times\mathbf{b} - \nabla p$$ Conservation of Momentum

$$\rho\partial_t\left(\frac{\mathbf{u}\cdot\mathbf{u}}{2} + T + \frac{\epsilon\mathbf{e}\cdot\mathbf{e}}{2} + \frac{\mathbf{b}\cdot\mathbf{b}}{2\mu}\right) + \rho\mathbf{u}\cdot\nabla\left(\frac{\mathbf{u}\cdot\mathbf{u}}{2} + T\right) = -\nabla\cdot(\mathbf{u}p) - \nabla\cdot\left(\mu^{-1}\mathbf{e}\times\mathbf{b}\right)$$ Conservation of Energy

$$(\partial_t + \mathbf{u}\cdot\nabla)\rho = -\rho\nabla\cdot\mathbf{u}$$ Conservation of Mass

$$\partial_t\epsilon\mathbf{e} + \mathbf{j} = \nabla\times\mu^{-1}\mathbf{b}$$ Ampere's Law

$$\partial_t\mathbf{b} = -\nabla\times\mathbf{e}$$ Faraday's Law

$$\mathbf{j} = \sigma(\mathbf{e} + \mathbf{u}\times\mathbf{b}) + \frac{\beta}{\sqrt{\mathbf{b}\cdot\mathbf{b}}}\mathbf{j}\times\mathbf{b}$$ Ohm's Law

$$\nabla\cdot\epsilon\mathbf{e} = \rho_c$$ Gauss' Law

$$\nabla\cdot\mathbf{b} = 0$$ Gauss' Law for Magnetism

Important Variables

$\mathbf{u}$ = velocity	$\mathbf{e}$ = electric field
$\mathbf{b}$ = magnetic flux density	T = thermal energy
ρ = mass density	ρ_c = charge density
$\mathbf{j}$ = current density	p = plasma pressure
σ = conductivity	β = Hall parameter
ϵ = (electric) permittivity	μ = (magnetic) permeability

Simplifying Assumptions

- **Low Magnetic Reynolds Number**
  Advection relatively unimportant, magnetic field should relax to a diffusive state.
- **The system is in equilibrium**
  All time derivatives are 0. We will lift this assumption after proof of concept.
- **The induced fields are very small**
  relative to the applied field, which we denote $\mathbf{b}_0$, therefore the plasma responds primarily to the applied field.
  This decouples the induced fields from the fluid flow.
- **The applied field is constant**
  throughout generator channel: $\mathbf{b}_0 = [0, 0, b_0]^T$

We choose a heuristic profile for $\mathbf{u}$ for now. Eventually a hydrostatic, or hydrodynamic system depending on $\mathbf{b}_0$ and $\mathbf{j}$ would be solved.

Static Formulation

This reduces the electromagnetics system as follows:
$\mathbf{u}, p, \rho, T, \mathbf{b}_0$ are fixed and independent of $\mathbf{b}, \mathbf{e}, \mathbf{j}$

$$\begin{cases} \nabla \times \mathbf{e} = 0 \\ \nabla \cdot \epsilon \mathbf{e} = \rho_c \end{cases}$$ Electrostatic System

$$\begin{cases} \nabla \times \mu^{-1} \mathbf{b} = \mathbf{j} \\ \nabla \cdot \mathbf{b} = 0 \end{cases}$$ Magnetostatic System

$$\mathbf{j} = \sigma(\mathbf{e} + \mathbf{u} \times \tilde{\mathbf{b}}) + \frac{\beta}{|\tilde{\mathbf{b}}|} \mathbf{j} \times \tilde{\mathbf{b}}$$ Ohm's Law

where $\tilde{\mathbf{b}} = \mathbf{b} + \mathbf{b}_0$.

Magnetostatic Problem

We formulate the magnetostatic problem in Coloumb Gauge:
$\nabla \cdot \mathbf{b} = 0 \implies \mathbf{b} = \nabla \times \mathbf{a}$, where $\mathbf{a}$ is the magnetic (vector) potential. We choose $\nabla \cdot \mathbf{a} = 0$.

Magnetostatic Problem

We formulate the magnetostatic problem in Coloumb Gauge:
$\nabla \cdot \mathbf{b} = 0 \implies \mathbf{b} = \nabla \times \mathbf{a}$, where $\mathbf{a}$ is the magnetic (vector) potential. We choose $\nabla \cdot \mathbf{a} = 0$.

$$\nabla \times \mu^{-1} \nabla \times \mathbf{a} = \mathbf{j}$$
$$\nabla \cdot \mathbf{a} = 0$$

Magnetostatic Problem

We formulate the magnetostatic problem in Coloumb Gauge:
$\nabla \cdot \mathbf{b} = 0 \implies \mathbf{b} = \nabla \times \mathbf{a}$, where $\mathbf{a}$ is the magnetic (vector) potential. We choose $\nabla \cdot \mathbf{a} = 0$.

$$\begin{aligned} \nabla \times \mu^{-1} \nabla \times \mathbf{a} &= \mathbf{j} \\ \nabla \cdot \mathbf{a} &= 0 \end{aligned}$$

However when we formulate the variational problem, we enforce the divergence condition weakly. Find $(\mathbf{a}, \lambda) \in \mathbf{H}^{\nabla\times} \times H^1$.

$$\begin{cases} (\nabla \times \mathbf{a}, \nabla \times \mathbf{c})_{\mathbf{L}^2} + (\nabla\lambda, \mathbf{c})_{L^2} = (\mathbf{j}, \mathbf{c})_{\mathbf{L}^2} \\ (\mathbf{a}, \nabla\eta)_{\mathbf{L}^2} = 0 \end{cases} \quad \forall(\mathbf{c}, \eta) \in \mathbf{H}^{\nabla\times} \times H^1 \qquad (*)$$

Magnetostatic Problem

We formulate the magnetostatic problem in Coloumb Gauge:
$\nabla \cdot \mathbf{b} = 0 \implies \mathbf{b} = \nabla \times \mathbf{a}$, where $\mathbf{a}$ is the magnetic (vector) potential. We choose $\nabla \cdot \mathbf{a} = 0$.

$$\nabla \times \mu^{-1} \nabla \times \mathbf{a} = \mathbf{j}$$
$$\nabla \cdot \mathbf{a} = 0$$

However when we formulate the variational problem, we enforce the divergence condition weakly. Find $(\mathbf{a}, \lambda) \in \mathbf{H}^{\nabla\times} \times H^1$.

$$\begin{cases} (\nabla \times \mathbf{a}, \nabla \times \mathbf{c})_{\mathbf{L}^2} + (\nabla \lambda, \mathbf{c})_{L^2} = (\mathbf{j}, \mathbf{c})_{\mathbf{L}^2} \\ (\mathbf{a}, \nabla \eta)_{\mathbf{L}^2} = 0 \end{cases} \quad \forall (\mathbf{c}, \eta) \in \mathbf{H}^{\nabla\times} \times H^1 \qquad (*)$$

- This problem is a well posed saddle point system. Further if $\nabla \cdot \mathbf{j} = 0$ then $\lambda = 0$.

Magnetostatic Problem

We formulate the magnetostatic problem in Coloumb Gauge:
$\nabla \cdot \mathbf{b} = 0 \implies \mathbf{b} = \nabla \times \mathbf{a}$, where $\mathbf{a}$ is the magnetic (vector) potential. We choose $\nabla \cdot \mathbf{a} = 0$.

$$\nabla \times \mu^{-1} \nabla \times \mathbf{a} = \mathbf{j}$$
$$\nabla \cdot \mathbf{a} = 0$$

However when we formulate the variational problem, we enforce the divergence condition weakly. Find $(\mathbf{a}, \lambda) \in \mathbf{H}^{\nabla\times} \times H^1$.

$$\begin{cases} (\nabla \times \mathbf{a}, \nabla \times \mathbf{c})_{\mathbf{L}^2} + (\nabla\lambda, \mathbf{c})_{L^2} = (\mathbf{j}, \mathbf{c})_{\mathbf{L}^2} \\ (\mathbf{a}, \nabla\eta)_{\mathbf{L}^2} = 0 \end{cases} \quad \forall (\mathbf{c}, \eta) \in \mathbf{H}^{\nabla\times} \times H^1 \qquad (*)$$

- This problem is a well posed saddle point system. Further if $\nabla \cdot \mathbf{j} = 0$ then $\lambda = 0$.
- Weak divergence imposes less regularity on $\mathbf{a}$ and also requires fewer degrees of freedom. [3].

Electrostatic Model

Note that $\nabla \times \mu^{-1}\mathbf{b} = \mathbf{j} \implies \nabla \cdot \mathbf{j} = 0$. Therefore

$$\nabla \cdot \mathbf{j} = \nabla \cdot \left(\sigma\Big(\mathbf{e} + \mathbf{u} \times (\mathbf{b} + \mathbf{b}_0)\Big) + \frac{\beta}{|\mathbf{b} + \mathbf{b}_0|}\mathbf{j} \times (\mathbf{b} + \mathbf{b}_0) \right) = 0$$

$$\implies \rho_c = -\nabla \cdot \epsilon\Big(\mathbf{u} \times (\mathbf{b} + \mathbf{b}_0) + \frac{\beta}{\sigma|\mathbf{b} + \mathbf{b}_0|}\mathbf{j} \times (\mathbf{b} + \mathbf{b}_0)\Big)$$

Electrostatic Model

Note that $\nabla \times \mu^{-1}\mathbf{b} = \mathbf{j} \implies \nabla \cdot \mathbf{j} = 0$. Therefore

$$\nabla \cdot \mathbf{j} = \nabla \cdot \left(\sigma\left(\mathbf{e} + \mathbf{u} \times (\mathbf{b} + \mathbf{b}_0)\right) + \frac{\beta}{|\mathbf{b} + \mathbf{b}_0|}\mathbf{j} \times (\mathbf{b} + \mathbf{b}_0)\right) = 0$$

$$\implies \rho_c = -\nabla \cdot \epsilon\left(\mathbf{u} \times (\mathbf{b} + \mathbf{b}_0) + \frac{\beta}{\sigma|\mathbf{b} + \mathbf{b}_0|}\mathbf{j} \times (\mathbf{b} + \mathbf{b}_0)\right)$$

By Helmholtz decomposition, as $\nabla \times \mathbf{e} = 0$ then $\mathbf{e} = \nabla\psi$, where ψ is the electric (scalar) potential. Using the above consistency condition we have the following electrostatic problem.

$$-\nabla \cdot \epsilon\nabla\psi = \nabla \cdot \epsilon\left(\mathbf{u} \times (\mathbf{b} + \mathbf{b}_0) + \frac{\beta}{\sigma|\mathbf{b} + \mathbf{b}_0|}\mathbf{j} \times (\mathbf{b} + \mathbf{b}_0)\right) \qquad (**)$$

Outline

Fixed Point Iteration

Ohm's law allows for a natural fixed point iteration:
$\mathbf{j} = \sigma(\mathbf{e} + \mathbf{u} \times \tilde{\mathbf{b}}) + \frac{\beta}{|\tilde{\mathbf{b}}|}\mathbf{j} \times \tilde{\mathbf{b}}$

begin
- $\mathbf{j}_1 = \sigma(\mathbf{u} \times \mathbf{b}_0)$;
- $n = 1$;
- **while** *error* $<$ *tolerance* **do**
  - Solve $(*)$ for $\mathbf{b}_n$ given data $\mathbf{j}_n$;
  - Solve $(**)$ for $\nabla\psi$ given data $\mathbf{b}_n, \mathbf{b}_0, \mathbf{j}_n$;
  - Update $\mathbf{j}_{n+1} = \sigma\left(\nabla\psi_n + \mathbf{u} \times (\mathbf{b}_0 + \mathbf{b}_n)\right) + \frac{\beta}{|\mathbf{b}_0+\mathbf{b}_n|}\mathbf{j}_n \times (\mathbf{b}_n + \mathbf{b}_0)$;
  - error $= \|\mathbf{j}_{n+1} - \mathbf{j}_n\|_{\mathbf{L}^2}$;
  - $n{+}{+}$;
- **end**

end

Initial guess $\sigma\mathbf{u} \times \mathbf{b}_0$ is current induced by applied field and fluid flow, it should be close to the bulk current.

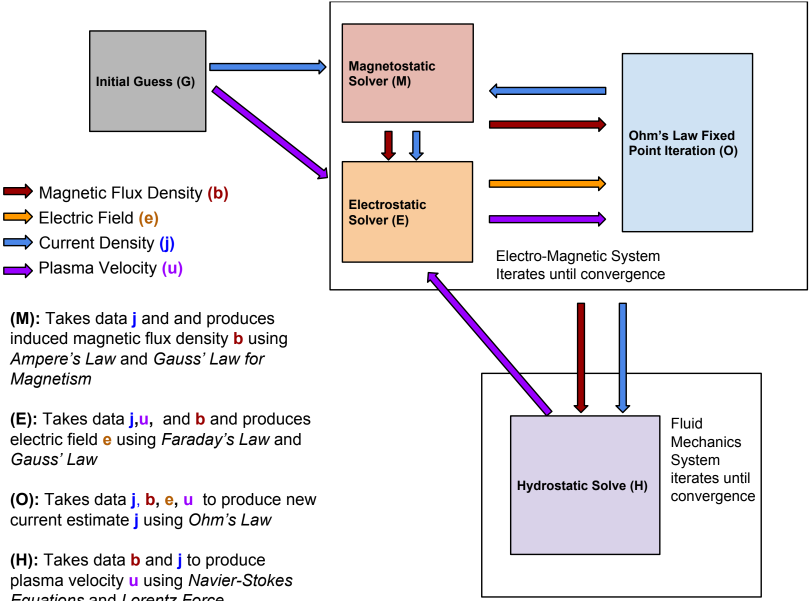

(M): Takes data **j** and and produces induced magnetic flux density **b** using *Ampere's Law* and *Gauss' Law for Magnetism*

(E): Takes data **j**,**u**, and **b** and produces electric field **e** using *Faraday's Law* and *Gauss' Law*

(O): Takes data **j**, **b**, **e**, **u** to produce new current estimate **j** using *Ohm's Law*

(H): Takes data **b** and **j** to produce plasma velocity **u** using *Navier-Stokes Equations* and *Lorentz Force*

(G): An initial guess **j** and **u**

Discretization

One of the important issues is to numerically maintain the $\nabla \cdot \mathbf{B} = 0$ (conservation of magnetic flux) condition, from Maxwell's equations, to avoid any unphysical effects. Therefore, we discretize with Mimetic Finite Differences (MFD) using a technique developed by K. Lipnikov, et al.

- MFD are a generalization of Yee-type staggered differences to general geometry.
- Difference operators are defined in terms of the Fundamental Theorem of Calculus, Divergence Theorem, and Stokes' Theorem.
- MFD describe a compatible discrete calculus which preserves standard range and kernel theorems.

$$\text{Range}(\nabla) = \text{Kernel}(\nabla\times) \qquad \text{Range}(\nabla\times) = \text{Kernel}(\nabla\cdot)$$

- Stability is inherited from the existence of a discrete Helmholtz Decomposition.

Discretizations of Interest

We are interested in compatible discretizations of, for example, certain low order Finite Element Methods. This provides the following relations

Discretizations of Interest

We are interested in compatible discretizations of, for example, certain low order Finite Element Methods. This provides the following relations

$$\begin{array}{ccccccc}
H^1 & \xrightarrow{\nabla} & \mathbf{H}^{\nabla\times} & \xrightarrow{\nabla\times} & \mathbf{H}^{\nabla\cdot} & \xrightarrow{\nabla\cdot} & L^2 \\
\downarrow & & \downarrow & & \downarrow & & \downarrow \\
\text{Trilinear} & \xrightarrow{GRAD_h} & \text{Nédélec} & \xrightarrow{CURL_h} & \text{Raviart–Thomas} & \xrightarrow{DIV_h} & \text{P.W. Const.} \\
\text{Vertices} & & \text{Edges} & & \text{Faces} & & \text{Cells}
\end{array}$$

Discretizations of Interest

We are interested in compatible discretizations of, for example, certain low order Finite Element Methods. This provides the following relations

$$\begin{array}{ccccccc} H^1 & \xrightarrow{\nabla} & \mathbf{H}^{\nabla\times} & \xrightarrow{\nabla\times} & \mathbf{H}^{\nabla\cdot} & \xrightarrow{\nabla\cdot} & L^2 \\ \downarrow & & \downarrow & & \downarrow & & \downarrow \\ \text{Trilinear} & \xrightarrow{GRAD_h} & \text{Nédélec} & \xrightarrow{CURL_h} & \text{Raviart–Thomas} & \xrightarrow{DIV_h} & \text{P.W. Const.} \\ \text{Vertices} & & \text{Edges} & & \text{Faces} & & \text{Cells} \end{array}$$

A well defined discrete calculus will allow for discrete proofs to follow easily from continuum proofs.

Further these methods are defined naturally on fairly general polyhedral meshes.

Magnetostatic Simulations

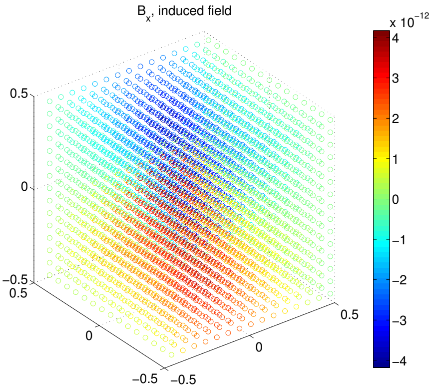

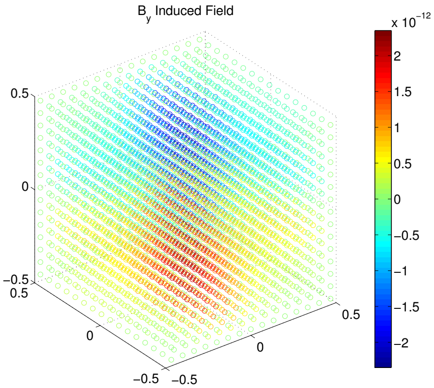

Outline

Features of the Arc

There are several features of an arc which we wish to be able to detect and quantify. In order to determine the feasibility of a **simulation-based parameter estimation**, we first test the sensitivity of the measurements to

- j_m: Total current in the system
- θ: Tilting of the current due to the Hall effect
- s: (Spread of) the distribution of current density.

We assume a parameterized current density profile **j** which has these features:

$$\mathbf{j}(x, y, z; j_m, \theta, s) = \frac{j_m}{\sqrt{2\pi s^2}} \mathbf{v} \exp\left(\frac{1}{2s^2} \left| (\mathbb{I} - \mathbf{v}\mathbf{v}^T) \begin{bmatrix} x \\ y \\ z \end{bmatrix} \right|^2 \right), \quad \mathbf{v} = \begin{bmatrix} \cos\theta \\ \sin\theta \\ 0 \end{bmatrix}$$

Sensitivity Results

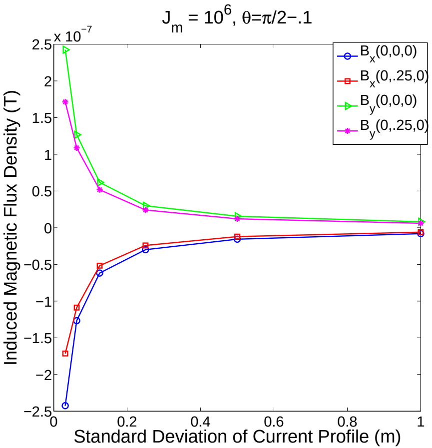

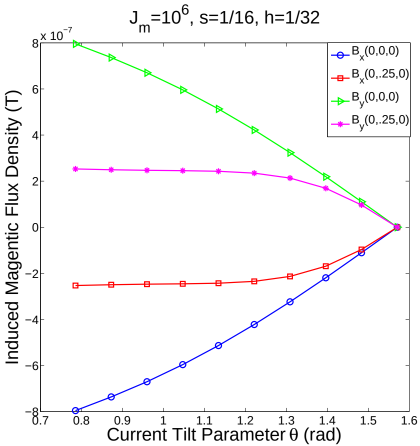

Outline

Conclusions

- We have formulated a (non-linear) static electromagnetic model for the MHD generator including the Hall effect.
- This reduced model is sensitive to characteristics of current density profiles.
- We have applied a mimetic finite difference method for the simulation of the model.
- We have formulated a nonlinear least squares parameter estimation problem for the detection of arcs using external (induced) magnetic flux density data.

Future Work

- Solve the inverse problem for the reduced model.
- Include quantification of uncertainty in measurements and estimation.
- Simulate the full (dynamic, coupled) forward problem.
- Solve the full inverse problem.

References

[1] K. Hauer and R. Potthast.
Magnetic tomography for fuel cells- current status and problems.
J.Phys.:Conf. Ser. 73 012008, pages 1–17, 2008.

[2] R. Kress, L. Kühn, and R. Potthast.
Reconstruction of a current distribution from its magnetic field.
Inv. Prob., 18:1127–1146, 2002.

[3] K. Lipnikov, G. Manzini, F. Brezzi, and A. Buff.
The mimetic finite difference method for the 3d magnetostatic field problems on polyhedral meshes.
J. Comp. Phys., 230:305–328, 2011.

[4] Richard Rosa.
Magnetohydrodynamic energy conversion.
McGraw-Hill, 1968.